A radiological and histochemical study of bone regeneration using the costal cartilage and artificial bone in rats

Miho Higeuchi

Nihon University Graduate School of Dentistry,

Major in Oral and Maxillofacial Surgery

(Directors: Prof. Yoshiyuki Yonehara, Assist.Profs. Shunsuke Namaki and Akihiko Furukawa)

Index

This thesis is composed of the following article and additional results of a mixture of costal cartilage and artificial bone in a bone defect (Figs. 3,7,8,11,12).

Higeuchi M, Namaki S, Furukawa A, Yonehara Y (2023) Radiological and histochemical study of bone regeneration using the costal cartilage in rats. J Oral Sci (in press)

Abstract

Purpose: Various materials, including autogenous and artificial bone grafts, are used for bone repair in the maxillofacial region. However, they all have both advantages and disadvantages. If bone repair with cartilage is possible, cartilage tissue can be used for hard-tissue reconstruction.

Methods: A 4-mm diameter bone defect was created in the right mandibular angle of rats. Cartilage, autologous bone, artificial bone and a mixture of cartilage and artificial bone were grafted into the defect. Computed tomography (CT) was performed to measure the increase in bone volume. Further histological evaluation of the grafted site was performed.

Results: At 12 weeks, CT show that bone formation in the cartilage group was comparable to that in the autogenous bone group. Histologically, in the artificial bone group and hybrid group, a clear boundary was observed between the existing bone and defect, whereas in the cartilage and autologous bone groups, laminar plate bone repair of the defect was observed.

Conclusion: The findings in this study suggest that bone reconstruction achieved with cartilage grafting is almost equivalent to that with autogenous bone grafting and that bone reconstruction using cartilage is clinically feasible. In future, if regenerated cartilage is successfully applied clinically, bone reconstruction using regenerated cartilage may be feasible.

Introduction

Trauma, inflammation, age-related bone resorption, and surgical resection of tumors result in maxillofacial bone defects. Bone loss results in inadequate bone support for prosthetic devices such as dentures and dental implants, leading to loss of functional aspects such as mastication, speech, and swallowing, and esthetic aspects such as lip support [1,2]. Autogenous bone grafts, such as vascularized bone grafts, free block bone grafts or particulate cancellous bone and marrow, have been used for reconstruction in cases with extensive jaw or alveolar bone defects with excellent results. Although reconstructive surgery improves the patient's quality of life, esthetically satisfactory reconstruction is difficult in the maxillofacial region, and intraoperative bone-graft reshaping is often required due to the complex geometry [3]. The disadvantages of autogenous bone grafting include the need for invasive surgery at the donor site and the limited amount of bone harvested [4,5]. Therefore various artificial bone substitutes have been developed [5], but their disadvantages include difficulty in implantation and failure to fuse properly with the host bone owing to the formation of fibrous tissue [6,7]. Thus, new reconstructive materials should be introduced considering the advantages and disadvantages of autogenous bone grafts and artificial materials [8,9].

Although various graft materials have been developed using regenerative medicine technology regeneration of bone-tissue structure has not yet been perfected. However, cartilage has been successfully cultured, and autologous chondrocyte implantation has been clinically used to

repair localized defects in the articular cartilage [10,11]. In fact, the costal cartilage is widely used in clinical practice to create frameworks for otoplasty [12,13], and Hoshi et al. achieved good mechanical strength and a three-dimensional shape for nasal deformity using implantable regenerated cartilage [14].

Cartilage, such as the costal and auricular cartilage, is be affected by aging and other causes [15]. However, few studies have described the process of cartilage ossification. Therefore, this study focused on cartilage ossification and hypothesized that hard-tissue reconstruction is possible through cartilage ossification. The purpose of this study was to conduct basic research on the possibility of using cartilage tissue for hard-tissue reconstruction and to observe morphological changes in the transition of the cartilage to bone.

Materials and Methods

Animals

Seven-week-old Wistar male rats (n = 35) weighing 150-170 g were used in each of the graft tissue types in this study. The animals were obtained from Sankyo Lab Service Co, and were kept in an animal house (22°C, 55% humidity, 12 h light/dark cycle). They were fed standard experimental feed and water. This study was approved by the Animal Experimentation Committee of Nihon University School of Dentistry. (AP21DEN011) Experiments were performed according to the institutional guidelines for the care and use of experimental animals described in the National Institutes of Health Guide for the Care and Use of Laboratory Animals. All efforts were made to minimize animal suffering and to reduce the number of animals used.

Surgery and Implanted Materials

All surgical procedures were performed after intraperitoneal administration of medetomidine hydrochloride (0.15 mg/kg, Domitor; Nippon Zenyaku Kogyo, Koriyama, Japan), midazolam (2 mg/kg, SANDOZ K. K, Kamiyama, Japan) and butorphanol tartrate (2.5 mg/kg, Butorphanol; Meiji Seika Pharma Co, Tokyo, Japan). The right lateral chest of the rats was shaved, infiltration anesthesia was induced with 2% lidocaine with epinephrine 1:80000 (Xylocaine; Astra Zeneca, Osaka, Japan), and an approximately 30-mm incision was made with a shear blade to expose the costal cartilage. Two costal cartilages, measuring approximately 5 mm, were extracted. The soft tissue was then returned to its original position and sutured using

a 5-0 nylon thread (BEAR Medic Corporation, Tokyo, Japan). The excised costal cartilage was trimmed to approximately 1 mm using a shear blade. Next, the area around the right mandibular angle was shaved and 2% lidocaine was injected subperiosteally. A skin incision of approximately 20 mm was made in the buccal region, and the masseter muscle and periosteum were incised to expose the mandibular angle. A bone defect was created in the mandibular angle using a 4-mm trephine bur (Implatex Corporation, Tokyo, Japan) under saline irrigation (Fig. 1A). In the autogenous costal cartilage graft group (CCG), the bone defect was filled with the harvested costal cartilage (Fig. 1B). In the autogenous bone graft group (AGG), the mandibular bone harvested at the time of defect creation was trimmed with scissors and grafted into the defect. Similarly, in the artificial bone graft group (ATG), the created mandibular-angle defect was filled with artificial bone (Cytrans Granules; GC Corporation, Tokyo, Japan). In the hybrid graft group (HBG), costal cartilage and artificial bone were mixed at a volume ratio of 1:1. In the control group (CG), no graft was placed in the defect. Finally, the soft tissue was returned to its original position and sutured using a 5-0 nylon thread to close the wound.

Computed Tomography

In CCG, AGG, ATG and CG, the right lateral mandibular angles of the rats were imaged using in vivo microcomputed tomography (R_mCT system; Rigaku Co., Tokyo, Japan) immediately after surgery and at 1, 4, 8, and 12 weeks. HBG was imaged immediately after surgery and at 12 weeks. At the time of imaging, rats were anesthetized with isoflurane (Mylan Pharmaceutical

Co., Ltd., Osaka, Japan). The rats were placed in the gantry, and radioscopy was performed in the coronal, sagittal, and axial planes to confirm that the created mandibular-angle defect was in the center of the visual field. The imaging conditions were as follows: magnification 6.7 ×, voxel size 30 μm × 30 μm × 30 μm, tube voltage 90 kV, tube current 100 μA, and irradiation time 17 sec. Three-dimensional images were constructed and 3by4viewer software (ver2.4, Kitasenju Radist Dental Clinic, Tokyo, Japan) was used to measure the bone volume from the voxel images. The region of interest was identified, and the bone volume within a cylindrical region (diameter, 4 mm; height 1.5 mm) was measured. The increase (green) and decrease (red) in voxels at each time point were calculated. Finally, the increase or decrease in bone volume was then calculated by subtracting the number of red voxels from that of the green voxels.

Statistical Analysis

The bone volume at 4, 8, and 12 weeks of CGG, AGG, ATG, and CG and the volume at 12 weeks of HBG are expressed as median, interquartile range (IQR). Data analyses were used with BellCurve (SSRI Co, Tokyo, Japan). Data were compared by the Kruskal-Wallis test, and multiple comparison tests were performed by the Scheffe method. Statistical significance was set at $P < 0.05$ and $P < 0.01$.

Histological Evaluation

In CCG, AGG, ATG and CG, mandibular specimens were extracted from rats at 1, 4, and 12 weeks after surgery. In HBG, specimens was extracted at 12 week. They were fixed in 4%

paraformaldehyde in phosphate buffer (FUJIFILM Wako Chemical, Osaka, Japan). The extracted specimens were decalcified using 10% ethylenediaminetetraacetic acid for 14 days at room temperature, dehydrated using ethanol in stages, and embedded in paraffin. Sections were prepared in the anteroposterior plane with a 3-μm thickness. All sections were stained with hematoxylin and eosin (HE). Additionally, in the CCG and HBG, sections were stained with 0.05％ toluidine blue (TB). The sections were observed under an optical microscope (CH3-CH; OLYMPUS Corporation, Tokyo, Japan).

Results

Evaluation of Computed Tomography Images

In CCG, the transplanted costal cartilage was observed as clearly demarcated radiopaque areas within the defect at 1 week (Fig. 2A). At 4 weeks, the radiopaque areas elongated, and the demarcation between the bone-defect edge and border of the costal cartilage became indistinct (Fig. 2B). At 12 weeks, radiopacity increased, and in the center of the defect, the bone and cartilage were indistinguishable (Fig. 2C).

In AGG, radiopaque areas were observed in the bony defect at 1 week (Fig. 2D). At 4 weeks, multiple bone grafts began to fuse, and continuity between the bone-defect edge and the autogenous bone was observed (Fig. 2E). At 12 weeks, the radiopaque area further increased, and the newly formed bone thickened (Fig. 2F).

In ATG, bone formation was observed at the bone-defect edge at 1 week (Fig. 2G). At 4 weeks, bone formation at the bone-defect edge increased, and some artificial bone granules were displaced within the defective area (Fig. 2H). Osteogenesis from the bone-defect edge continued at 12 weeks. However, no bone formation was observed between the artificial bone granules (Fig. 2I).

In CG, a small the radiopaque area was observed at the defect site at 1 week (Fig. 2J). At 4 weeks, bone formation was observed at the bone-defect edge (Fig. 2K). Although the radiopaque areas increased, the defect persisted at 12 weeks. (Fig. 2L).

In HBG showed radiopacity increased from the bone-defect edge and radiopacity increased of the costal cartilage at 12 weeks. However, the defect remained and there was no bone formation between the grafts (Fig. 3).

Quantitative Analysis Using Computed Tomography

The bone volume increased in a time-dependent manner until 12 weeks in CCG, AGG, and CG. In ATG, bone volume increased until 8 weeks, but decreased at 12 weeks.

In CG, CCG, and AGG, bone volume at 4, 8, and 12 weeks was 1.50 mm^3 (1.43-1.76 mm^3), 4.52 mm^3 (3.46-5.95 mm^3), and 4.49 mm^3 (3.50-6.59 mm^3); 2.36 mm^3 (1.77-3.02 mm^3), 4.42 mm^3 (3.65-5.30 mm^3), and 5.99 mm^3 (5.47-6.35 mm^3); and 2.48 mm^3 (1.70-3.12 mm^3), 5.34 mm^3 (4.30-6.17 mm^3), and 6.24 mm^3 (6.10-6.69 mm^3), respectively. Comparison of the bone volumes at 4, 8, and 12 weeks between CCG, AGG, and CG showed that the increase in bone volume in CCG and AGG was significantly greater than that in CG. There were no significant differences between CCG and AGG ($P = 0.509$) (Figs. 4, 5)

In ATG, bone volume at 4, 8, and 12 weeks was 2.63 mm^3 (2.26-2.75 mm^3), 2.71 mm^3 (2.40-2.85 mm^3), 2.06 mm^3 (1.69-2.56 mm^3). In the comparison of CG, CCG, and ATG, the increase in bone volume at 4 weeks was significantly different between CG and CCG ($P = 0.002$), but no significant difference was observed between CCG and ATG ($P = 0.195$). At 8 weeks, significant differences were found between CG and CCG ($P = 0.005$) and between CCG and ATG ($P = 0.025$). At 12 weeks, the CCG showed more than twice bone augmentation compaired

to the ATG (Figs. 4, 6).

In HBG, bone volume at 12 weeks was 3.33 mm^3 (2.96 - 3.46 mm^3). Comparison of the bone volume in CCG, ATG, and HBG showed significant differences between CCG and ATG ($P < 0.001$) and between CCG and HBG ($P = 0.049$) (Figs. 7, 8).

Histological findings

In CCG, HE staining showed infiltration of inflammatory cells around the grafted cartilage in the bone defect at 1 week (Fig. 9A). At 4 weeks, a layer of bone tissue was observed around the cartilage. Chondrocyte hypertrophy was also observed (Fig. 9B). At 12 weeks, the cartilage tissue reduced, and the cartilage were surrounded by bone tissue. Remaining chondrocytes are hypertrophied, and the cartilage matrix reduced. Some new lamellar bone formation was observed (Fig. 9C). TB staining showed metachromasia in the transplanted cartilage at 1 week (Fig. 10A). At 4 weeks, the cartilage were more intensely stained (Fig. 10B). At 12 weeks, the specimens showed the same level of metachromasia as at 4 weeks, but the area where the grafted cartilage was completely replaced by bone did not show metachromasia (Fig. 10C).

In AGG, at 1 week, the grafted bone was surrounded by granulation tissue, and the boundary with the existing bone transection was clear (Fig. 9D). At 4 weeks, reticular bone was formed from the bone-defect edge (Fig. 9E). At 12 weeks, laminar bone formation was observed in continuity with the existing bone-defect edge (Fig. 9F).

In ATG, at 1 week, the artificial bone granules were surrounded by fibrous tissue (Fig. 9G).

At 4 weeks, bone growth was observed from the bone-defect edge and the granules were surrounded by fibrous tissue (Fig. 9H). At 12 weeks, the granules were surrounded by fibrous tissue. Some granules enclosed the bone that had grown beyond the bone defect edge. No significant morphological changes were observed in the remaining artificial bone granules. (Fig. 9I).

In CG at 1 week, infiltration of inflammatory cells was observed in the defect (Fig. 9J). At 4 and 12 weeks, fibrous granulation tissue was observed in the defect, and the boundary between the existing bone and the defect was well defined (Figs. 9K, L).

In HBG, HE staining showed bone formation from the bone-defect edge at 12 weeks and showed hypertrophy of chondrocytes. Some of the grafted cartilage was in close proximity to the new bone formed from the bone-defect edge, but some was encased in fibrous tissue. Similarly, artificial bone granules were encased in fibrous tissue (Fig. 11). TB staining showed metachromasia in the transplanted grafted cartilage. However, the outer circumference of the cartilage showed less tendency to exhibit metachromasia (Fig. 12).

Discussion

This study evaluated morphological changes in the costal cartilage grafted to the bone. Radiological observations showed bone formation from the bone-defect edge at 1 week in AGG, although the grafted bone remained intact and retained its morphology. CCG showed calcification around the cartilage at the center of the defect and calcification at the bone-defect edge. At 4 weeks, bone formation from the existing bone progressed in AGG, the grafted bone itself actively underwent resorption and bone formation, and bone volume increased. In CCG, computed tomography (CT) showed vigorous bone formation in the gaps between and around the grafted cartilage, and areas of bone defects were covered. at 12 weeks, AGG showed nearly continuous new bone formation. Bone repair comparably in CCG and AGG.

Hamada et al. created 5-mm segmental defects in the femurs of rats and transplanted cancellous bone taken from the iliac bone [16]. Radiographic evaluation revealed changes suggestive of osteogenesis at 2 weeks, and continuity between the existing and grafted bone was observed at 4 weeks. Moreover, changes suggestive of osteogenesis were most pronounced at 8 weeks. Williams et al. created closed fractures in the femurs of mice and histologically observed the healing process over time [17]. After the fracture, chondrocytes appeared and hypertrophied, formed calcified cartilage, and callus formation was observed. They reported that as remodeling progressed, bone resembling cortical bone was observed. In the present study, AGG showed bone formation from the existing bone and inflammatory cells around the grafted

bone at 1 week. In CCG, new bone formation from the existing bone and some calcification around the grafted cartilage were observed. In AGG, the bone defects were repaired with reticular bone by 4 weeks. In CCG, cartilage tissue persisted in the defect, but good osteogenesis around the cartilage and cartilage calcification were observed. In AGG, the reticular bone observed at 4 weeks morphologically changed to lamellar bone at 12 weeks, and the bone defect was repaired with mature bone. In CGG, cartilage tissue reduced, and the area around the cartilage tissue was covered with newly formed bone, including lamellar bone. Moreover, in some areas, cartilage fragments were completely calcified. In this study, the histological picture observed in CGG was similar to that of the bone healing process reported by Williams et al. [17], suggesting that the process of ossification of the grafted cartilage follows a process similar to that of fracture healing.

In this study, HE staining revealed pulverized hyaline cartilage in CCG at 1-week. At 4 weeks, chondrocyte hypertrophy and enlargement of the cartilage lacunae compared with that at 1 week were observed. At 12 weeks, the chondrocytes and cartilage lacunae further enlarged and the cartilage matrix reduced. TB is excellent for staining cartilage containing proteoglycans, because it stains acidic mucopolysaccharides. Residual cartilage were darkly stained at weeks 1, 4, and 12; however, the area where the grafted cartilage was completely replaced by bone did not show metachromasia. Tubular bone grows through a process called endochondral ossification [18]. Mackie et al. reported that a cartilage model is initially formed, followed by

differentiation into chondrocytes and chondrocyte hypertrophy. Simultaneously, an extracellular matrix is secreted, mineralization proceeds, and causes bone progression [19]. In this study, the grafted chondrocytes hypertrophied, and calcification from the surrounding area was observed. Thus, the same process of endochondral ossification was recapitulated.

The 4-mm diameter bone defect created in the mandibular angle in this study was a critical-diameter bone defect [20,21] and was a suitable model to determine if other methods of replacements would be useful. However, there are differences in the timing of observations between this study and the report by Hamada et al. [16]. In the present study, the process of repair of bone defects by ossification of the grafted cartilage was similar to that of the autologous bone graft.

AGG and CGG were compared using CT subtraction images; there was no statistically significant difference in bone mass gain at 4, 8, and 12 weeks (Figs. 4, 5). This indicates that cartilage and bone have equal regenerative capacities. In contrast, when comparing CCG and ATG, there was no significant difference in bone formation at 4 weeks, but CCG showed significantly better bone formation at 8 and 12 weeks (Figs. 4, 6). Once artificial bone was filled into the bone defect, the bone defect area decreased. Therefore, there was no difference between CCG and ATG at 4 weeks; however, at 8 and 12 weeks, osteogenesis occurred in CGG, but not in ATG, resulting in a significant difference. Comparing CCG, ATG, and HBG after 12 weeks, bone formation was significantly better in CCG than in ATG and HBG (Figs. 7, 8). The cartilage

implanted alone was better than mixed with artificial bone.

Elsheikh et al. reported that differences in carbonate apatite porosity affect the internal growth rate of bones [22]. They created 6-mm diameter, 3-mm long cylindrical defects in the distal part of rabbit femurs, implanted carbonate apatite with pore volumes of 30% and 15%, and observed the defects at 4 and 12 weeks [22]. Their study reported that at 4 weeks, boundaries with the existing bone could be radiologically distinguished in both, the carbonate apatite block with 30% pore volume and carbonate apatite block with 15% pore volume groups. However, at 12 weeks, the carbonate apatite block with 30% pore volume was resorbed and replaced by cancellous new bone, while that with 15% pore volume had a clear boundary with the existing bone. In this study, at 1 week, the morphology of the implanted granules was retained in ATG. At 4 weeks, no calcification was observed around the artificial bone, the morphology of the grafted artificial bone was maintained, and new bone formation from the existing bone alone was observed. At 12 weeks, bone formation from the existing bone was observed, but more than half of the artificial bone remained, and more bone defects remained than those in the other two groups.

In this study, bone formation from the bone-defect edge was observed histologically in ATG; however, none such bone formation was observed in the gaps between the artificial bone particle at 12 weeks. The artificial bone used in this study was composed mainly of carbonate apatite, which is a dense granule without pores. Elsheikh et al. reported that at 12 weeks, the

carbonate apatite block with 30% pore volume had a blurred boundary with the existing bone, while the carbonate apatite block with 15% pore volume had a clear boundary with the existing bone. Elsheikh et al report that differences in carbonate apatite porosity affect the internal growth rate of bone [22]. Thus, if the porosity of the artificial bone is altered, better bone formation may be observed than that in the present study. Although artificial bone was found to be useful as a filling material, its bone-forming capacity was much lower than those of bone and cartilage. The results of this study suggest that cartilage grafting is more useful than artificial bone grafting or mixture of artificial bone and cartilage for bone formation.

In this study, the osteogenic potential of cartilage was almost equal to that of autologous bone. The primary goal of this study, in terms of duration of observation, is to clarify the scope of differences between autologous bone and cartilage as bone graft materials. Twelve weeks later, a similar bone repair was observed in autologous bone and cartilage. Therefore, this period was defined as the observation result determination period. It suggests that both cartilage grafts and bone grafts are viable options for bone reconstruction. When bone grafting is performed, resorption and addition of the grafted bone occur due to bone metabolism. In cartilage grafts, bone differentiation is considered to occur in the grafted cartilage itself, while bone induction occurs from the bone defect edge due to the cartilage. It is a fact that the periosteum has good osteogenic capacity. In the model of this study, the periosteum was preserved. When the bone defect was created. The bone defect was again covered with periosteum after grafted. Therefore,

osteogenic capacity from the periosteum was preserved. On the other hand, when cartilage was transplanted subcutaneously, its properties were maintained [23]. Therefore, it is believed that the periosteum may affect cartilage ossification. To reconstruct a small defect, cartilage can be harvested from the auricle. In addition, the costal cartilage can be harvested if reconstruction of a large bone defect is required. Costal cartilage is selected when the amount of graft is large, such as in a mandibular segmentectomy. Transplantation of auricle cartilage is considered feasible for maxillary anterior bone augmentation. In such transplants, the periosteum should be preserved if possible. Compared to harvesting the iliac bone for autogenous bone grafting, costal cartilage harvesting is associated with fewer complications, such as postoperative pain. Clinical trials indicate that regenerated cartilage grafts can effectively treat deep cartilage defects [10]. Based on the results of this study, hard-tissue reconstruction using cartilage is feasible and that bone reconstruction using regenerated cartilage transplantation may be achievable in the future if regenerated cartilage becomes available for clinical application.

Acknowledgments

This study was supported by the Sato Fund and Dental Research Center of Nihon University School of Dentistry.

Conflict of interest

The authors declare that they have no competing interests.

References

1. Depprich R, Naujoks C, Lind D, Ommerborn M, Meyer U, Kübler NR et al. (2011) Evaluation of the quality of life of patients with maxillofacial defects after prosthodontic therapy with obturator prostheses. Int J Oral Maxillofac Surg 40, 71-79.
2. Handschel J, Hassanyar H, Depprich RA, Ommerborn MA, Sproll KC, Hofer M et al. (2011) Nonvascularized iliac bone grafts for mandibular reconstruction-requirements and limitations. In Vivo 25, 795-799.
3. Batstone MD (2018) Reconstruction of major defects of the jaws. Aust Dent J 63, 108-113.
4. Schmidt AH (2021) Autologous bone graft: Is it still the gold standard? Injury 52, 18-22.
5. Trombetta RP, Knapp EK, Awad HA (2021) A mouse femoral ostectomy model to assess bone graft substitutes. Methods Mol Biol 2230, 75-89.
6. Noori A, Ashrafi SJ, Vaez-Ghaemi R, Hatamian-Zaremi A, Webster TJ (2017) A review of fibrin and fibrin composites for bone tissue engineering. Int J Nanomedicine 12, 4937-4961.
7. Qi J, Yu T, Hu B, Wu H, Ouyang H (2021) Current biomaterial-based bone tissue engineering and translational medicine. Int J Mol Sci 22, 10233.
8. Friesenbichler J, Maurer-Ertl W, Sadoghi P, Pirker-Fruehauf U, Bodo K, Leithner A (2014) Adverse reactions of artificial bone graft substitutes: lessons learned from using tricalcium phosphate geneX®. Clin Orthop Relat Res 472, 976-982.
9. Zhao R, Yang R, Cooper PR, Khurshid Z, Shavandi A, Ratnayake J (2021) Bone grafts and

substitutes in dentistry: a review of current trends and developments. Molecules 26, 3007.

10. Brittberg M, Lindahl A, Nilsson A, Ohlsson C, Isaksson O, Peterson L et al. (1994) Treatment of deep cartilage defects in the knee with autologous chondrocyte transplantation. N Engl J Med 331, 889-895.
11. Hosih K, Fujihara Y, Asawa Y, Nishizawa S, Kanazawa S, Sakamoto T et al. (2013) Recent trends in cartilage regenerative medicine and its application to oral and maxillofacial surgery. Oral Sci Int 10, 15-19.
12. Bly RA, Bhrany AD, Murakami CS, Sie KC (2016) Microtia reconstruction. Facial Plast Surg Clin North Am 24, 577-591.
13. Yotsuyanagi T, Yamashita K, Yamauchi M, Nakagawa T, Sugai A, Kato S et al. (2019) Establishment of a standardized technique for concha-type microtia-how to incorporate the cartilage frame into the remnant ear. Plast Reconstr Surg Glob Open 7, e2337.
14. Hoshi K, Fujihara Y, Saijo H, Kurabayashi K, Suenaga H, Asawa Y et al. (2017) Three-dimensional changes of noses after transplantation of implant-type tissue-engineered cartilage for secondary correction of cleft lip-nose patients. Regen Ther 7, 72-79.
15. Kusafuka K, Yamaguchi A, Kayano T, Takemura T (2001) Ossification of tracheal cartilage in aged humans: a histological and immunohistochemical analysis. J Bone Miner Metab 19, 168-174.
16. Hamada T, Matsubara H, Hikichi T, Shimokawa K, Tsuchiya H (2021) Rat model of an

autologous cancellous bone graft. Sci Rep 11, 18001.

17. Williams JN, Li Y, Valiya Kambrath A, Sankar U (2018) The generation of closed femoral fractures in mice: a model to study bone healing. J Vis Exp 138, 58122.
18. Wuelling M, Vortkamp A (2009) Transcriptional networks controlling chondrocyte proliferation and differentiation during endochondral ossification. Pediatr Nephrol 25, 625-631.
19. Mackie EJ, Ahmed YA, Tatarczuch L, Chen KS, Mirams M (2007) Endochondral ossification: how cartilage is converted into bone in the developing skeleton. Int J Biochem Cell Biol 40, 46-62.
20. Miller MQ, McColl LF, Arul MR, Nip J, Madhu V, Beck G et al. (2019) Assessment of hedgehog signaling pathway activation for craniofacial bone regeneration in a critical-sized rat mandibular defect. JAMA Facial Plast Surg 21, 110-117.
21. Zhang W, Shi W, Wu S, Kuss M, Jiang X, Untrauer JB et al. (2020) 3D printed composite scaffolds with dual small molecule delivery for mandibular bone regeneration. Biofabrication 12, 035030.
22. Elsheikh M, Kishida R, Hayashi K, Tsuchiya A, Shimabukuro M, Ishikawa K (2022) Effects of pore interconnectivity on bone regeneration in carbonate apatite blocks. Regen Biomater 9, rbac010.
23. Belaldavar BP, Mudhol RS, Dhorigol V, Belaldavar C, Desai S, Garg R et al. (2015) Study

of outcome of an implanted autologous auricular cartilage: a preliminary experimental research in rabbits. Indian J Otolaryngol Head Neck Surg 68, 11-15.

Figures

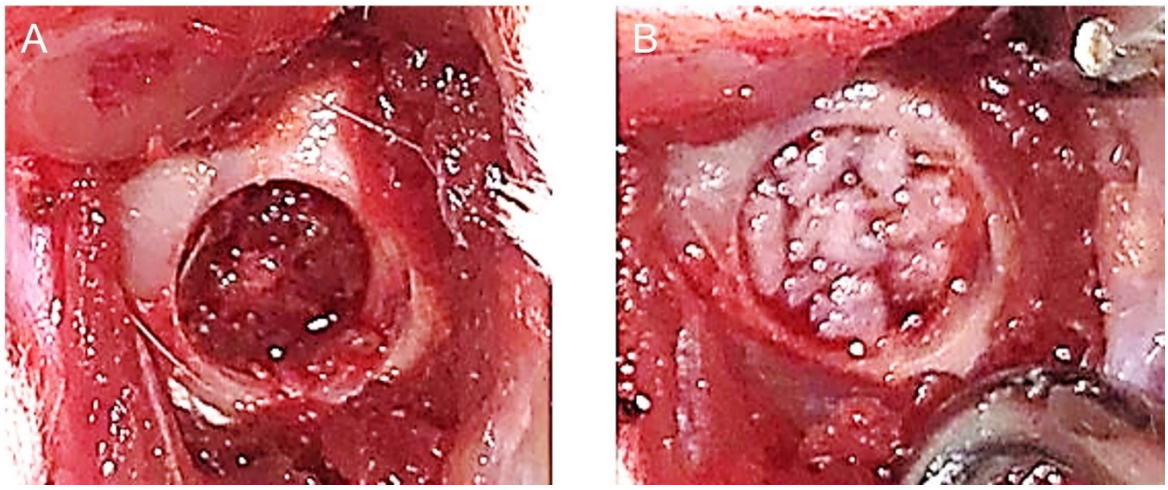

Fig. 1 intraoperative images

A: A 4-mm diameter bone defect has been created in the right mandibular angle of a rat.

B: Trimmed costal cartilage has been grafted into the created bone defect.

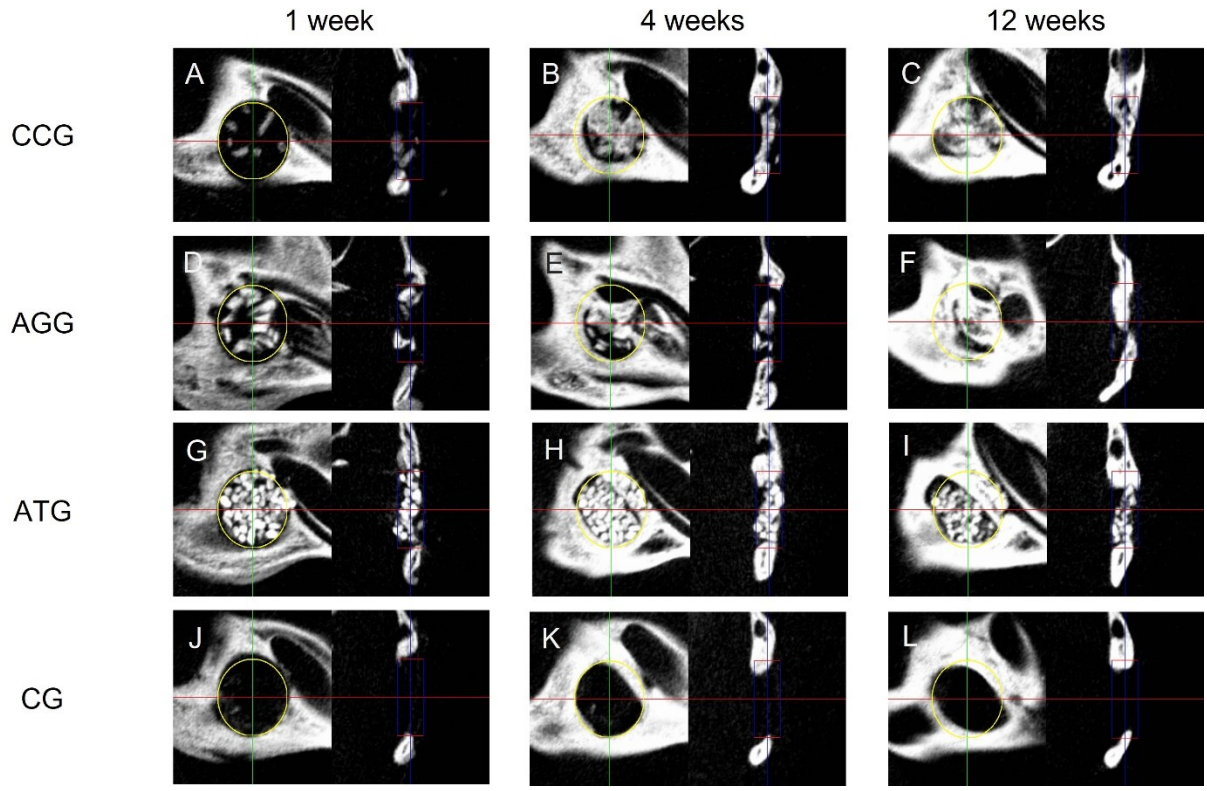

Fig. 2 Representative sagittal (left) and coronal (right) computed tomography images

In CCG, the radiopacity of the transplanted costal cartilage increases from the 1st 12th week. AGG also shows increase in graft radiopacity and continuity with the existing bone over time. In ATG, the radiopacity of the existing bone increases over time; however, no significant change is observed in the artificial bone. In CCG, the radiopacity from the existing bone increases over time and bone defect remained.

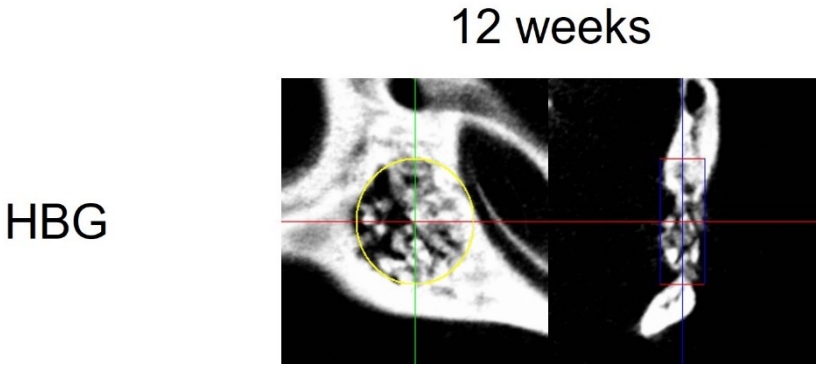

Fig. 3 Representative sagittal (left) and coronal (right) computed tomography images in HBG.

The boundary between the existing bone and the graft was clear and the defect remained.

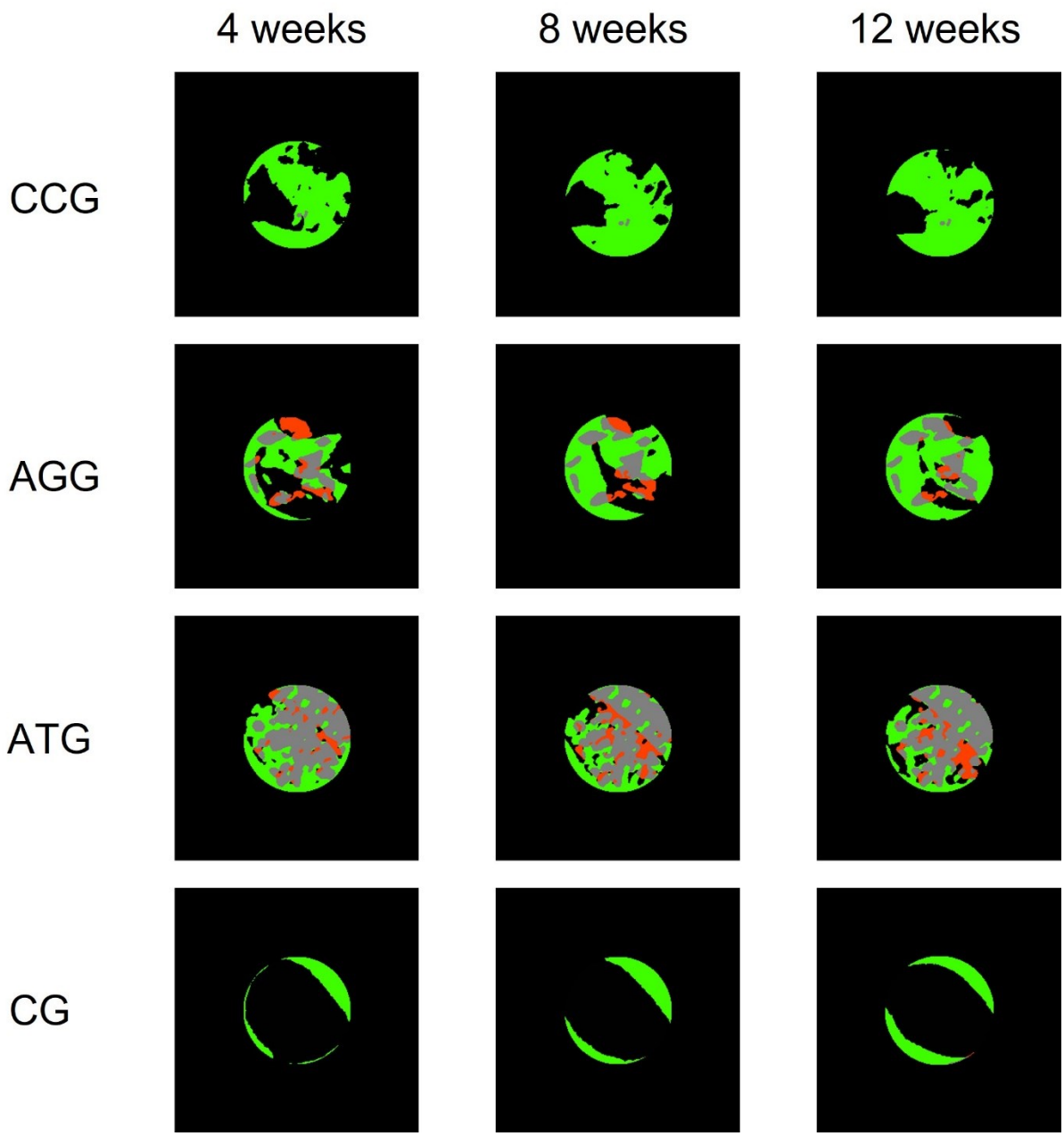

Fig. 4 Measurement of increase in bone quantity

Images of the defect sites obtained using 3by4viewer software. Green: newly mineralized tissue; Red: absorbed bone; gray, no change

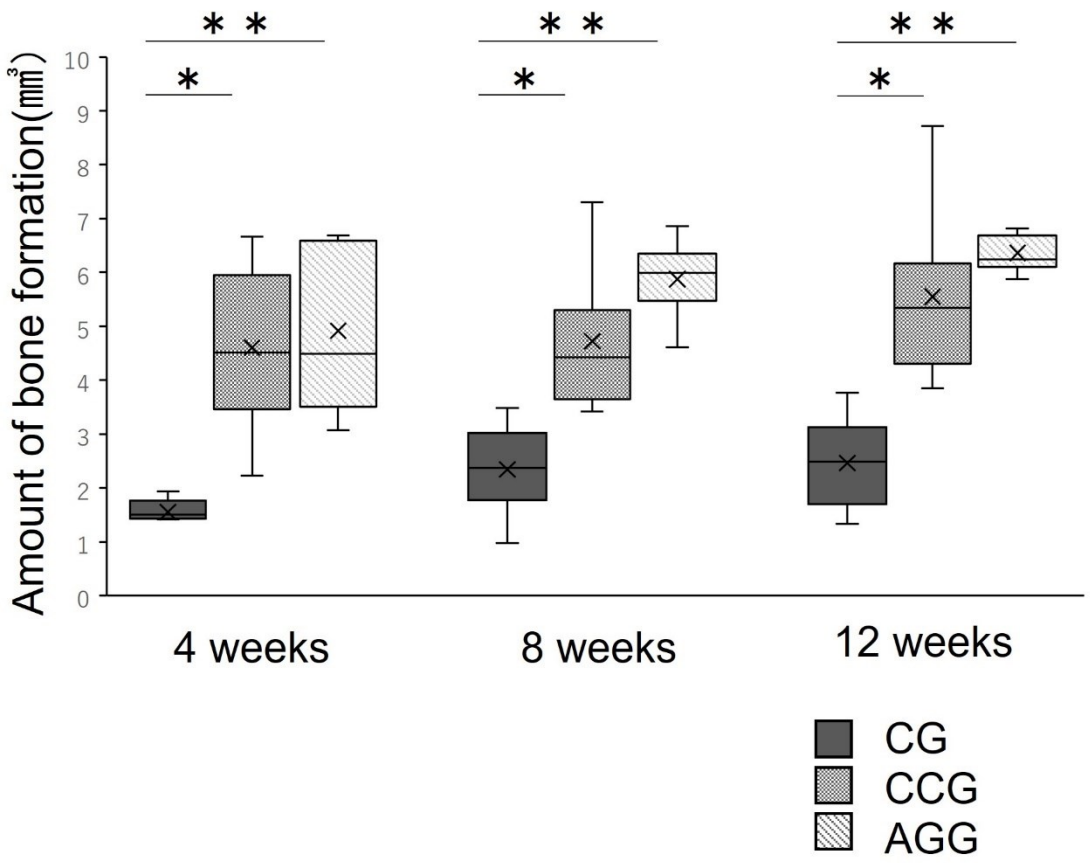

Fig. 5 Graph comparing the increase in bone volume immediately after surgery and at 4, 8, and 12 weeks in CG, CCG, and AGG. Data are presented as median, IQR. The interior lines in the box-and-whisker plot diagram indicate the median and the x indicates the mean. (*$P < 0.05$, **$P < 0.01$).

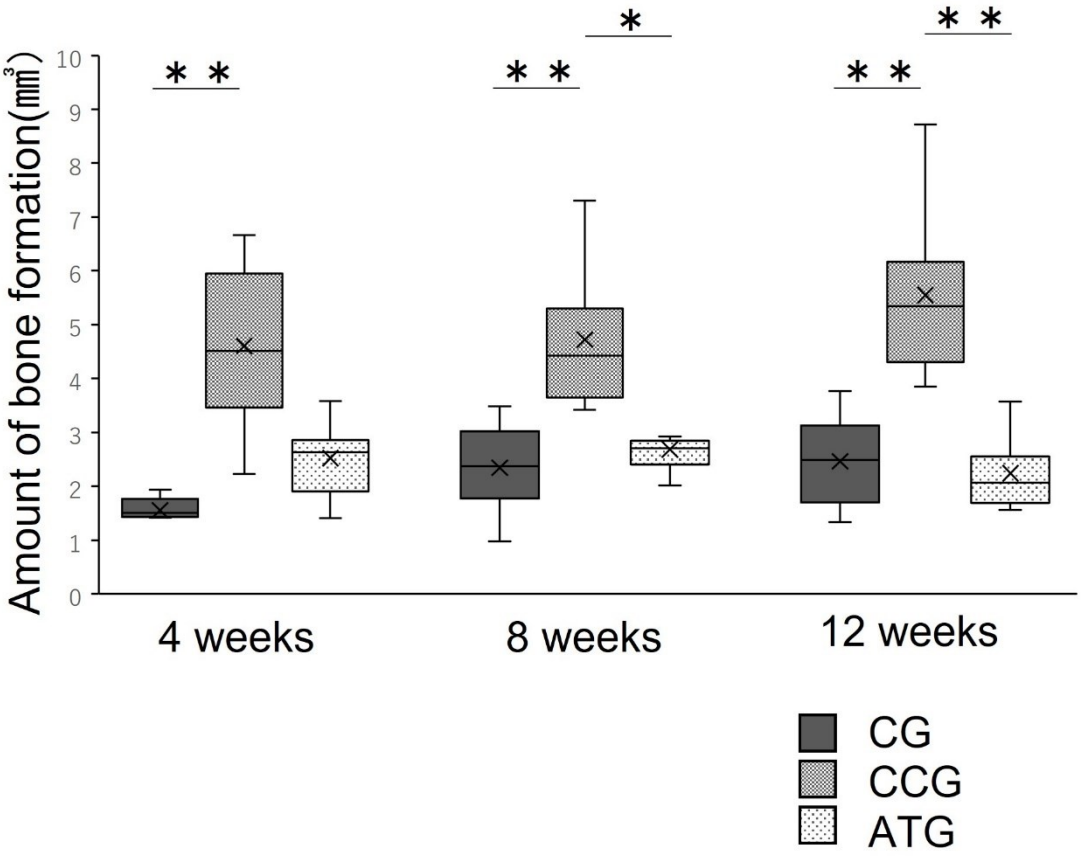

Fig. 6 Graph comparing the increase in bone volume immediately after surgery and at 4, 8, and 12 weeks in CG, CCG, and ATG. Data are presented as median, IQR. The interior lines in the box-and-whisker plot diagram indicate the median and the x indicates the mean. (*$P < 0.05$, **$P < 0.01$).

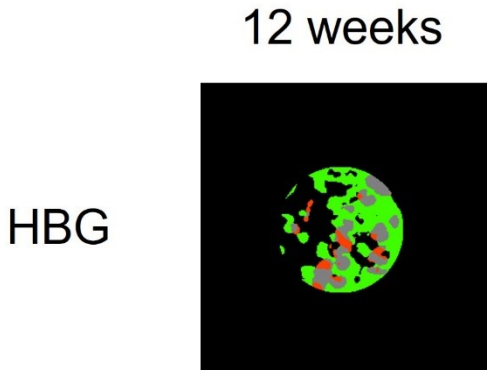

Fig. 7 Measurement of increase in bone quantity

Images of the defect sites obtained using 3by4viewer software. Green: newly mineralized tissue; Red: absorbed bone; gray, no change

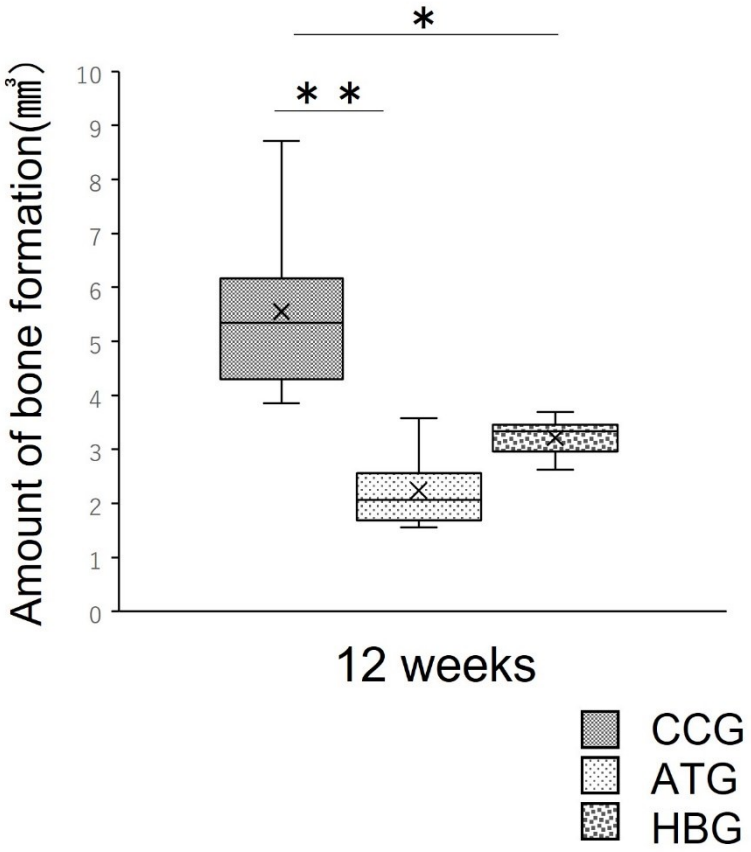

Fig. 8 Graph comparing the increase in bone volume immediately after surgery and at 12 weeks in CCG, ATG and HBG. Data are presented as median, IQR. The interior lines in the box-and-whisker plot diagram indicate the median and the x indicates the mean. (*P < 0.05, **P < 0.01).

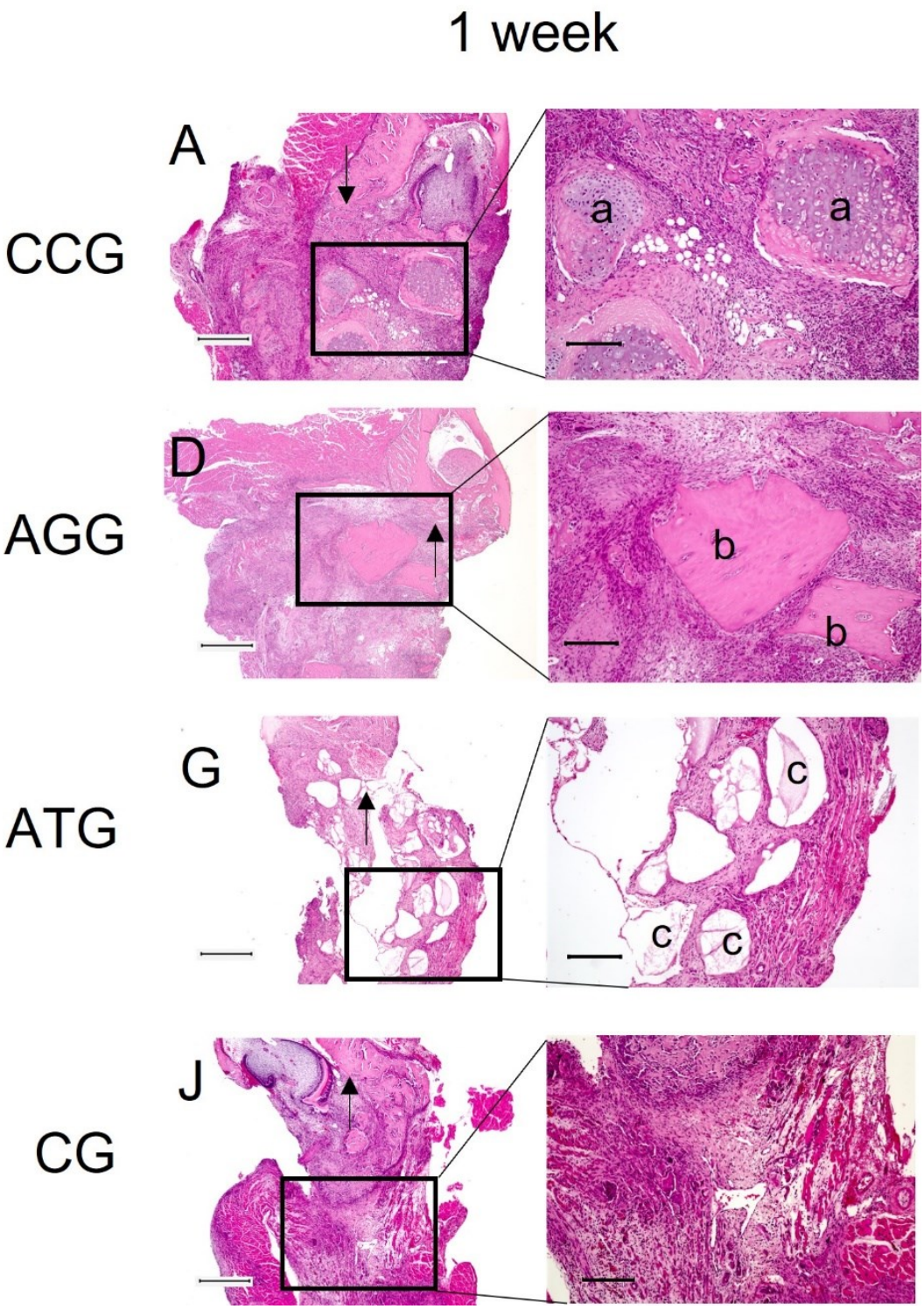

(continued)

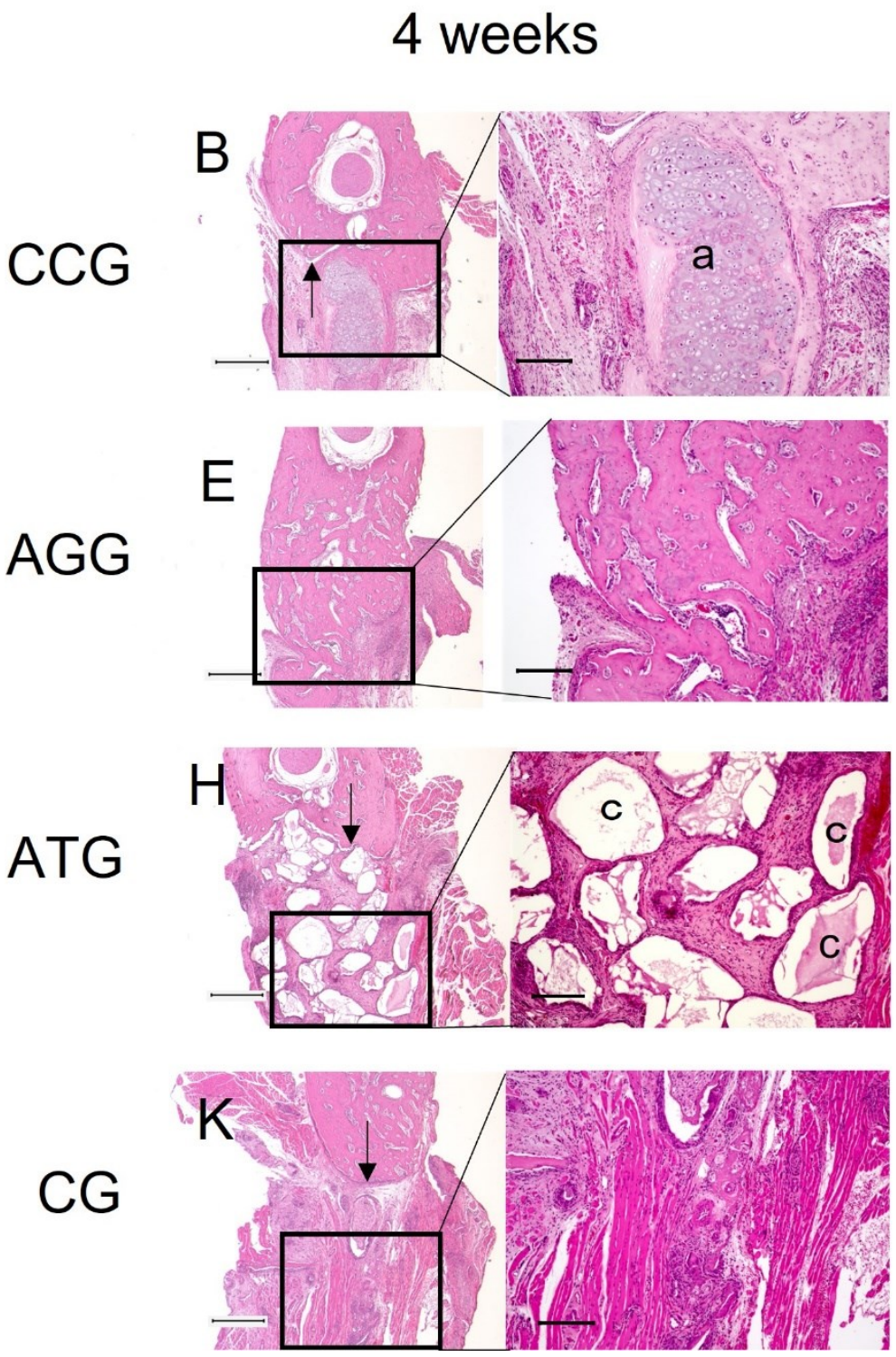

(continued)

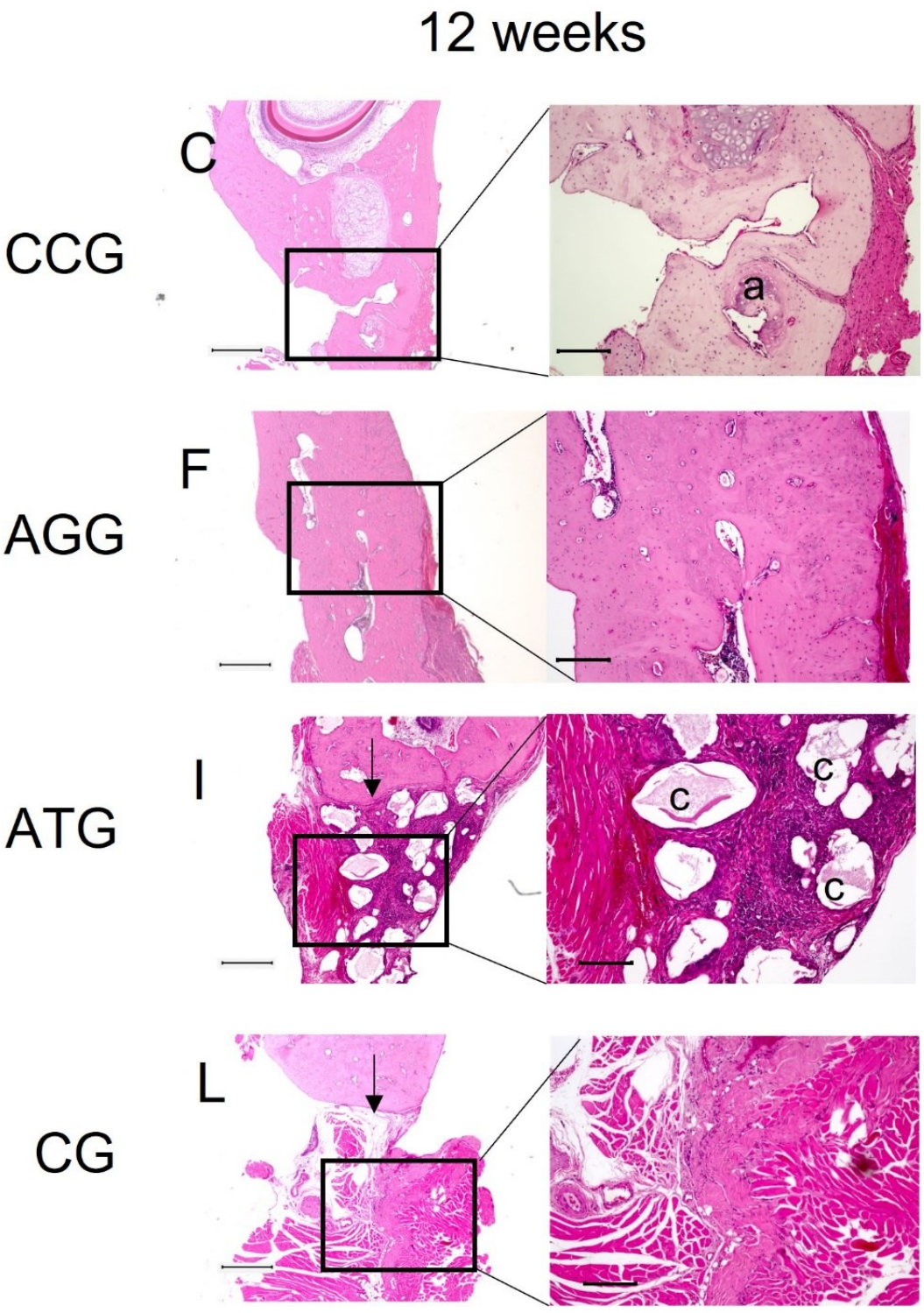
12 weeks
CCG
C
a
AGG
F
ATG
I
c
c
c
CG
L

Fig. 9 Hematoxylin and eosin stained sections of the boundary between the existing bone and defect

The figure on the left shows the boundary between the existing bone and the defect. Scale bar, 500 μm. The figure on the right is an enlargement of the enclosed area in the figure on the left. The perimeter of the graft is shown. Scale bar, 200 μm. Arrows, boundary between the existing bone and defect. a, trimmed costal cartilage; b, trimmed autogenous bone; c, artificial bone

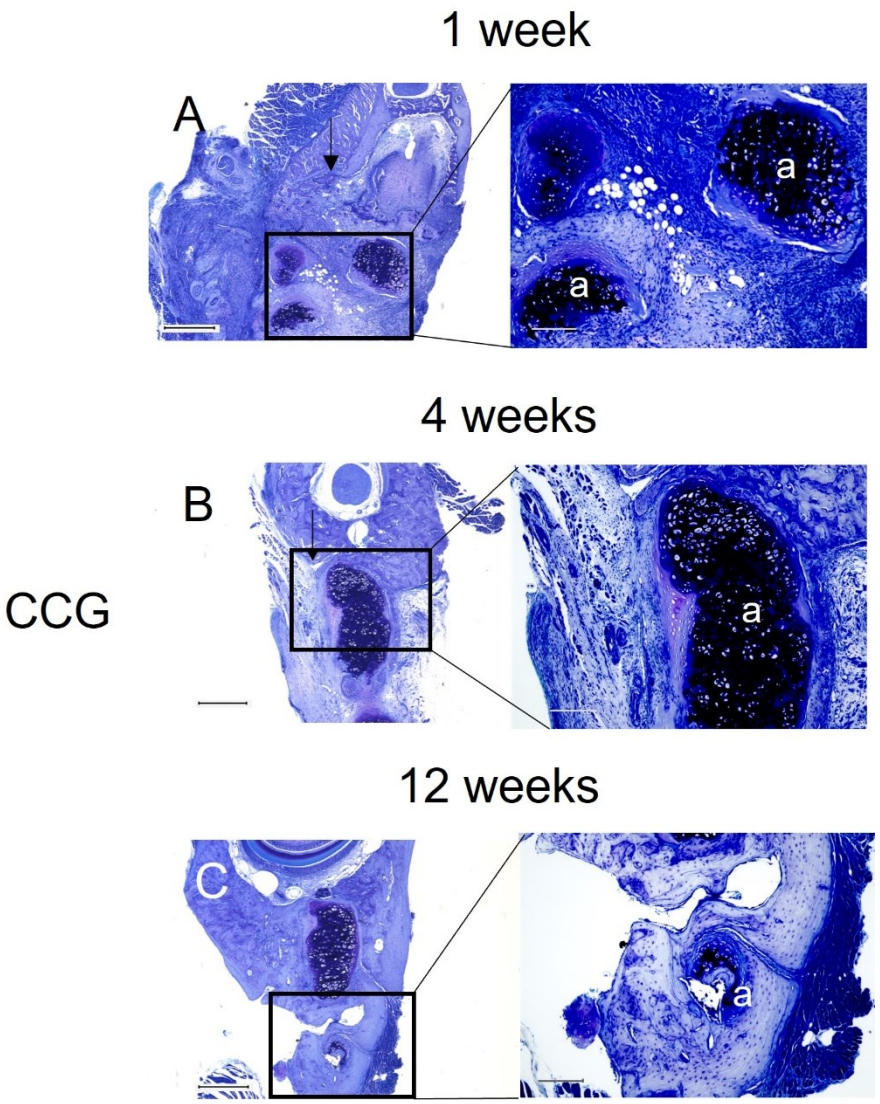

Fig. 10 Toluidine blue stained sections of the boundary between the existing bone and defect

The figure on the left shows the boundary between the existing bone and the defect. Scale bar, 500 μm. The figure on the right is an enlargement of the enclosed area in the figure on the left. The perimeter of the graft is shown. Scale bar, 200 μm. Arrows, boundary between the existing bone and defect. a, trimmed costal cartilage

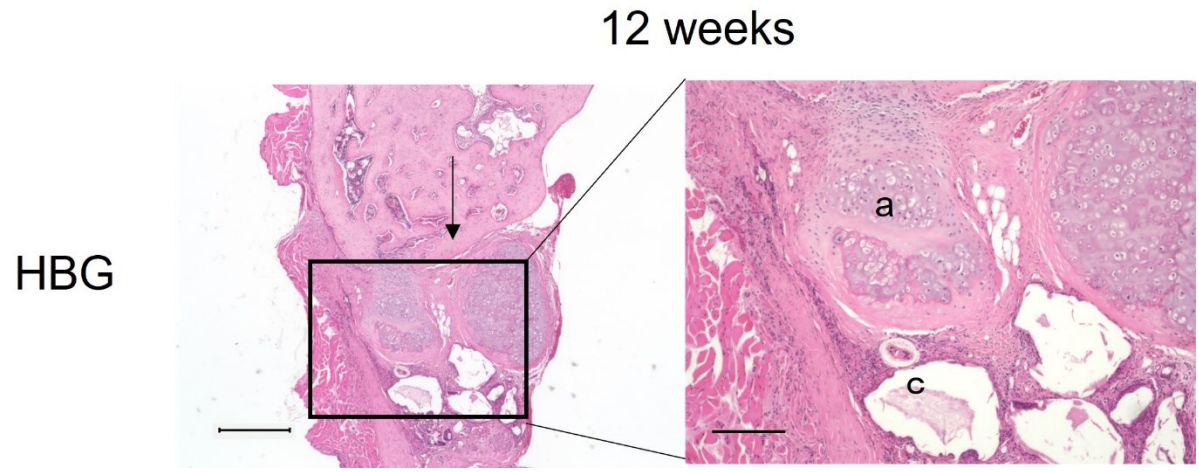

Fig. 11 Hematoxylin and eosin stained sections of the boundary between the existing bone and defect

The figure on the left shows the boundary between the existing bone and the defect. Scale bar, 500 μm. The figure on the right is an enlargement of the enclosed area in the figure on the left. The perimeter of the graft is shown. Scale bar, 200 μm. Arrows, boundary between the existing bone and defect. a, trimmed costal cartilage; c, artificial bone

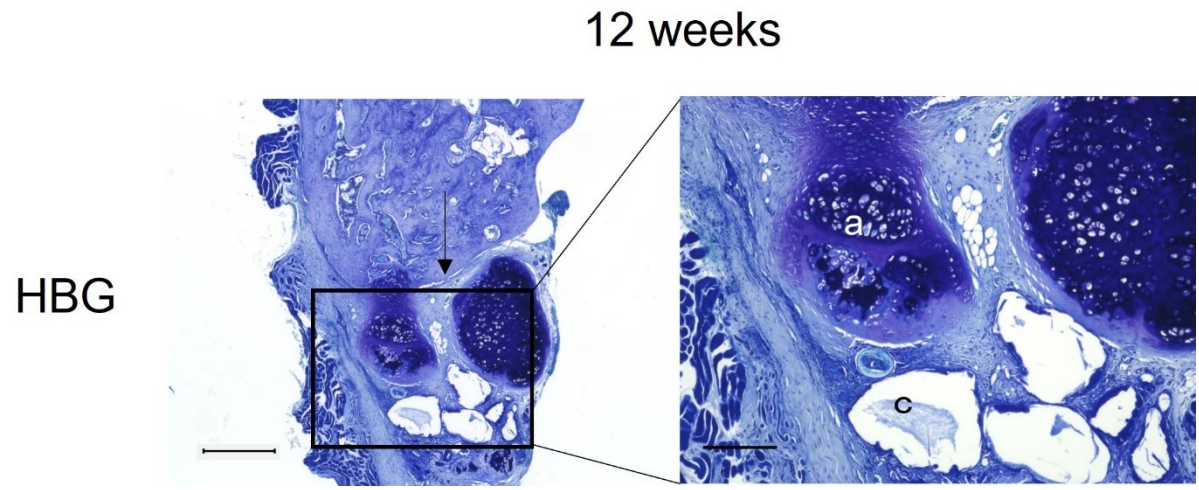

Fig. 12 Toluidine blue stained sections of the boundary between the existing bone and defect

The figure on the left shows the boundary between the existing bone and the defect. Scale bar, 500 μm. The figure on the right is an enlargement of the enclosed area in the figure on the left. The perimeter of the graft is shown. Scale bar, 200 μm. Arrows, boundary between the existing bone and defect. a, trimmed costal cartilage; c, artificial bone